Cell, Vol. 89, 773–779, May 30, 1997, Copyright ©1997 by Cell Press

Mutations Involving the Transcription Factor CBFA1 Cause Cleidocranial Dysplasia

S. Mundlos,[1,2,13] F. Otto,[7,13] C. Mundlos,[3,4] J. B. Mulliken,[5] A. S. Aylsworth,[8] S. Albright,[8] D. Lindhout,[9] W. G. Cole,[10] W. Henn,[11] J. H. M. Knoll,[3,4] M. J. Owen,[12] R. Mertelsmann,[7] B. U. Zabel,[1] and B. R. Olsen[2,6]

[1]Kinderklinik
Klinikum der Johannes-Gutenberg-Universität
55101 Mainz, Germany
[2]Department of Cell Biology
[3]Division of Genetics
Children's Hospital
[4]Department of Pathology
Beth Israel Deaconess Medical Center
[5]Division of Plastic Surgery
Children's Hospital
Harvard Medical School
Boston, Massachusetts 02115
[6]Harvard-Forsyth Department of Oral Biology
Harvard School of Dental Medicine
Boston, Massachusetts 02115
[7]Abteilung Hämatologie-Onkologie
Klinikum der Albert-Ludwigs-Universität
79106 Freiburg, Germany
[8]Department of Genetics
Division of Genetics and Metabolism
University of North Carolina at Chapel Hill
Chapel Hill, North Carolina 27599
[9]MGC-Department of Clinical Genetics
Erasmus University
Rotterdam, The Netherlands
[10]Division of Orthopaedics
The Hospital for Sick Children
Toronto, Ontario, Canada, M5G 1X8
[11]Institut für Humangenetik
Universität des Saarlandes
Homburg, Germany
[12]Imperial Cancer Research Fund
London WC2A 3PX, United Kingdom

Summary

Cleidocranial dysplasia (CCD) is an autosomal-dominant condition characterized by hypoplasia/aplasia of clavicles, patent fontanelles, supernumerary teeth, short stature, and other changes in skeletal patterning and growth. In some families, the phenotype segregates with deletions resulting in heterozygous loss of *CBFA1*, a member of the *runt* family of transcription factors. In other families, insertion, deletion, and missense mutations lead to translational stop codons in the DNA binding domain or in the C-terminal transactivating region. In-frame expansion of a polyalanine stretch segregates in an affected family with brachydactyly and minor clinical findings of CCD. We conclude that *CBFA1* mutations cause CCD and that heterozygous loss of function is sufficient to produce the disorder.

[13]These authors contributed equally to this work.

Introduction

Hereditary skeletal disorders comprise a large group of human malformation syndromes (for review, see Mundlos and Olsen, 1997a, 1997b). The causative mutations can either affect the entire skeleton, with resulting dwarfism, or lead to an altered number, size, or shape of particular bones. Cleidocranial dysplasia (CCD) is a disorder exhibiting defective endochondral and intramembranous bone formation (see Jones, 1997). Typical features include hypoplasia/aplasia of clavicles, patent fontanelles (Figure 1), Wormian bones (additional cranial plates caused by abnormal ossification of the calvaria), supernumerary teeth, short stature, and other skeletal changes. The abnormalities suggest that the responsible gene is not only active during early patterning, as implied by the absence (clavicles) and/or addition (teeth and cervical ribs) of skeletal elements, but is also important for fetal and postnatal growth. A transcription factor in the *runt* family, CBFA1, is essential for osteoblastic differentiation, as described in an accompanying paper (Otto et al., 1997 [this issue of *Cell*]). Inactivation of one *Cbfa1* allele in mice is sufficient to produce skeletal defects that are essentially identical to those found in human CCD. In addition, *Cbfa1* is deleted in a radiation-induced murine mutant (Ccd) that has a CCD-like phenotype (Selby and Selby, 1978). The human and murine mutant syndromes map to syntenic regions on chromosomes 6p21 and 17, respectively (Mundlos et al., 1995; Otto et al., 1997).

Here, we report that *CBFA1* mutations are associated with human CCD. We describe deletions involving the *CBFA1* locus and alterations in the *CBFA1* gene that lead to synthesis of an inactive gene product. The results indicate that CBFA1 is essential for skeletal morphogenesis and prove that heterozygous loss of one *Cbfa1* allele in the mouse is a model for human cleidocranial dysplasia.

Results

CCD Locus and *CBFA1* Are Colocalized on Chromosome 6p21

We recently described linkage to markers on chromosome 6p21 in two kindreds with CCD (Mundlos et al., 1995). Three additional large families, totaling 62 individuals and including 39 affected members, showed linkage to the 6p locus (data not shown). Recombination events at markers D6S452 and D6S282 defined the region of interest (Figure 2A). The region was covered with a total of 14 yeast artificial chromosomes (YACs). Three known genes were identified within the contig: *TCTE1*, a testis-expressed gene (Kwiatkowski et al., 1991); *MUT*, methylmalonyl CoA mutase (Ledley et al., 1988); and *CBFA1*, a transcription factor belonging to the *runt* family (Levanon et al., 1994). *CBFA1* mapped within the middle of the contig, close to the proximal end of YAC 948G7 (Figure 2A). A member of the *runt* family had previously been described as a bone-specific nuclear–

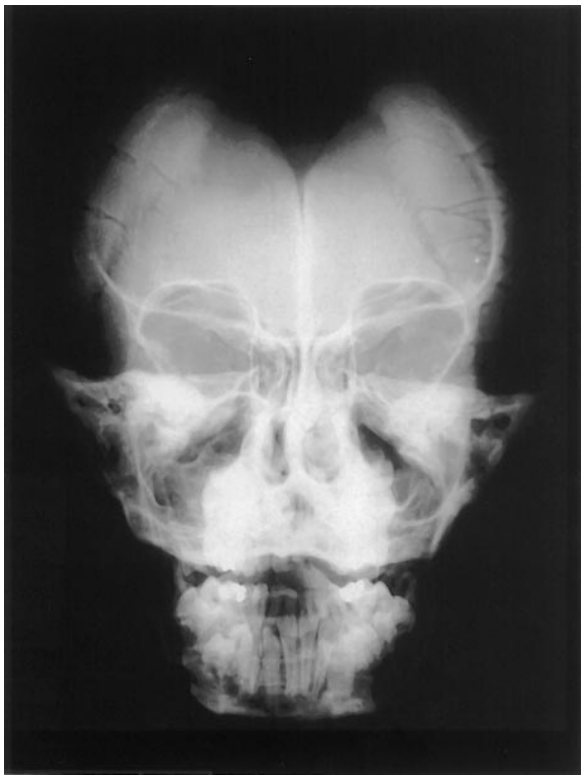

Figure 1. Ten-Year-Old Boy with Failed Closure of Anterior/Posterior Fontanelles and Sagittal Suture

Note multiple parietal Wormian bones.

matrix binding transcription factor (Merriman et al., 1995). This made *CBFA1* a reasonable candidate gene for CCD.

Large Deletions Including *CBFA1* in Unrelated CCD Patients

In our previous paper (Mundlos et al., 1995), we described hemizygosity for D6S459 in a family with CCD (CCD-O), suggesting a deletion that likely includes the *CCD* gene (Figure 2B). Therefore, YACs were tested by fluorescent in situ hybridization (FISH) for loss of heterozygosity in one affected individual in this family. YACs 939E12, 948G7, 886A4, and 818A7 gave a hybridization signal of reduced intensity on one chromosome, indicating a partial deletion. In contrast, YACs 898D3 and 747H9 did not hybridize on one chromosome but gave a normal signal on the other, whereas YACs 769A9 and 761E9 gave normal signals on both chromosomes. These results confirmed the presence of a deletion and enabled us to narrow the region of interest to approximately 1.5 Mb (Figure 2B).

We also examined a patient (CCD-H) with a pericentric inversion involving chromosome 6p21q16 (Nienhaus et al., 1993). Clinically, he had moderate mental retardation in addition to CCD. FISH demonstrated a similar breakpoint distally with partial deletion of YAC 886A4 as in family CCD-O. A proximal extension of the deletion was suggested by the absence of a signal with YAC 939E12 (Figure 2B) on the inverted chromosome.

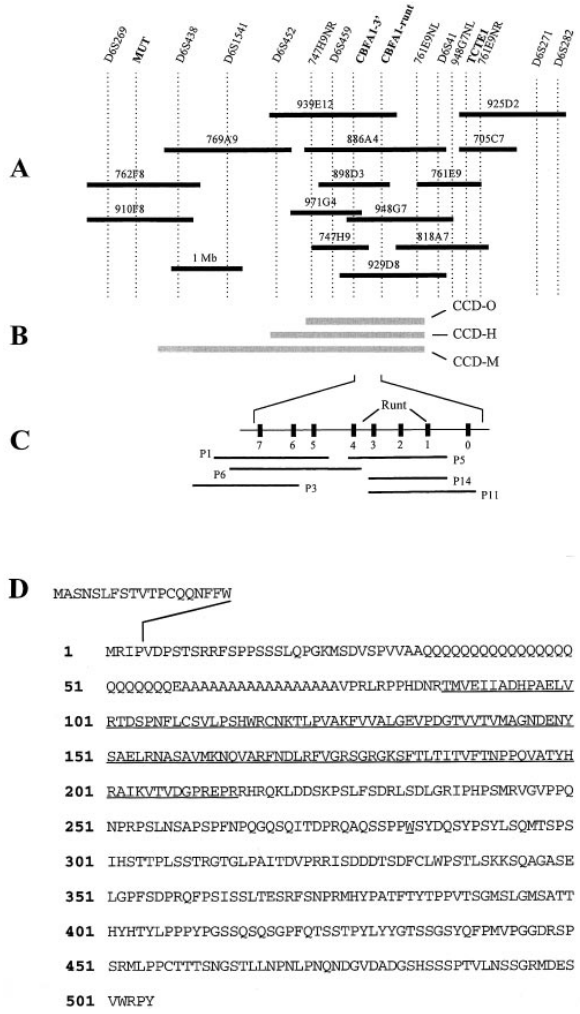

Figure 2. Physical Map of CCD Locus, Deletions in Three CCD Pedigrees, Location and Exon Structure of *CBFA1* Gene, and Amino Acid Sequence of CBFA1

(A) Overlapping YAC clones covering CCD locus. Markers used to map locus and order YACs are shown at top of figure. Known genes (*MUT*, *CBFA1*, and *TCTE1*) that mapped to YAC contig are indicated in bold. -NL and -NR refer to cloned and sequenced end regions of specific YACs used for ordering. Telomere is to right and centromere is to left.

(B) Deleted regions in family O (CCD-O) and in patients H (CCD-H) and M (CCD-M) have similar distal boundaries. Proximal boundary of CCD-H deletion not tested and should be considered tentative.

(C) Location of *CBFA1* relative to YAC contig and exon structure of gene. Six PACs covering entire gene are indicated. *runt* domain in *CBFA1* is encoded by exons 1–3 (exons counted from 5′ end of gene). Exon 0 contains an alternative translation start site.

(D) Numbers on left indicate amino acids in translated sequence counted from methionine residue in exon 1. Amino acid sequence of *runt* domain underlined. The alternative translation start and N-terminal sequence in exon 0 are shown on top. Affected son of family CCD-J has G-to-A transition at codon 283 (corresponding tryptophan residue is underlined) that converts TGG codon to TGA (stop) codon.

Finally, we examined patient M (CCD-M). An investigation at the age of five years revealed, in addition to CCD, broad thumbs, dislocated radial heads, conductive hearing loss, and minor developmental retardation.

Chromosome analysis showed a pericentric inversion of chromosome 6p21q, with possible duplication of part of 6p21. FISH demonstrated a large deletion with a proximal break-point involving YAC 762F8, since this YAC gave a reduced signal on one chromosome (Figure 2B). YAC 769A9 and YAC 939E12 gave no signal, whereas YAC 886A4 and YAC 948G7 gave a reduced signal. This indicated that the distal breakpoint is similar to that of CCD-O and CCD-H.

Characterization of the Human *CBFA1* Gene

To search for *CBFA1* mutations in other families with CCD, we first cloned and sequenced the human gene. A human PAC library (Reference Library, RZPD; Lehrach et al., 1990) was screened using probes from the mouse *Cbfa1* gene. Six of the isolated clones, P1(LLNPL704 H04166), P3(LLNPL704M18222), P5(LLNPL704O09256), P6(LLNPL704E1923Q), P11(LLNPL704K01244Q13), and P14(LLNPL704F01264Q13) are shown in Figure 2C. They cover the entire *CBFA1* gene (Figure 2C) and are contained within YAC 898D3 (data not shown), suggesting that the entire *CBFA1* gene is deleted in family O and in patients H and M (Figure 2). Using a combination of RT–PCR with RNA from EBV-transformed lymphoblasts and direct sequencing of PAC clones, we amplified and sequenced the *CBFA1* coding sequence. Eight exons were identified by comparison with the murine *Cbfa1* and human *CBFA2* and *CBFA3* sequences. The human CBFA1 amino acid sequence is shown in Figure 2D. In contrast to CBFA2 (AML1) and CBFA3 (AML2), the other members of the *runt* family, CBFA1 contains a region of 23 uninterrupted glutamine residues followed by 17 uninterrupted alanine residues on the N-terminal side of the *runt* domain.

Based on a comparison with the human *CBFA2* gene (Miyoshi et al., 1995), two alternative translational-initiator codons can be identified. A cryptic 3′ splice site in exon 1 of *CBFA1* allows the generation of two transcripts encoding protein products with different N-terminal amino acid sequences. One product would start with a sequence (MRIPV) encoded by exon 1 (Figure 2D). The alternative product would contain a sequence from exon 0 spliced to an aspartic acid residue at position 6 (Figure 2D). While an N-terminal sequence corresponding to that encoded by exon 0 has been found in murine *Cbfa1* cDNA (Ducy et al., 1997 [this issue of *Cell*]), the MRIPV sequence, encoded by exon 1, has not been detected. This may reflect differences in the utilization of splice sites in the human and murine genes.

Mutations within *CBFA1* Segregate with the Phenotype in Three Unrelated CCD Families

To identify mutations in *CBFA1*, we amplified fragments from genomic DNA and analyzed RT–PCR products with RNA from EBV-transformed lymphoblasts. Double bands in two (G and B) families were revealed by agarose gel electrophoresis of amplification products.

The affected child in family G (CCD-G) showed a band of slower mobility in addition to the wild-type band, whereas the unaffected parents had only the wild-type band (Figure 3A). The amplification products of child and parents were subcloned, and individual clones were sequenced. The larger band in the affected child was

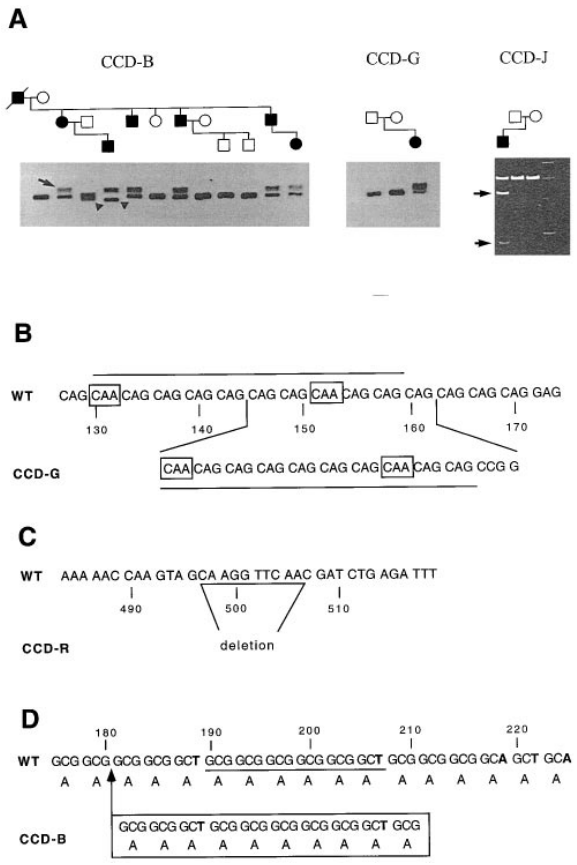

Figure 3. Analyses of Mutant Regions in CCD Pedigrees

(A) Gel analyses of PCR-amplified mutant regions in pedigrees CCD-B, CCD-G, and CCD-J. Larger band (arrow) in affected members of CCD-B represents in-frame duplication of 30 bp within the polyalanine region of CBFA1. Spouse of an affected family member and his son show additional shorter band (triangles) identified as a polymorphic 18 bp deletion within polyalanine region. Affected daughter of family CCD-G has a 16 bp insertion within polyglutamine region; parents have only wild-type allele. Affected son in family CCD-J has G-to-A transition in codon 283. This nucleotide change creates a new restriction site for MboI, which cuts PCR-amplified sequence of affected allele into two fragments (arrows); amplified DNA from unaffected parents is not cut. Molecular weight size markers shown on right.

(B) Frame-shift mutation in polyglutamine stretch in family CCD-G. Mutant sequence differs from that of wild type in that nt 145–162 (counted from methionine residue in exon 1) are replaced by a longer sequence (bottom). Comparison of the positions of CAA codons (indicated by boxes) in wild type and mutant sequences suggests that mutation involved duplication of sequence between nt 130 and 159 (indicated by horizontal line) and addition of CCGG tetranucleotide.

(C) Frame-shift mutation in *runt* domain in CCD-R. Deletion of 10 nt between nt 497 and 506 causes stop codon downstream of mutation.

(D) Nucleotide and amino acid sequence of polyalanine stretch in CBFA1. Imperfections in GCG repeats indicated in bold letters. The 18 bp deletion leading to 11 alanine polymorphism is underlined. The 30 bp duplication in family CCD-B and possible insertion point are shown below.

caused by insertion of 16 nt within the polyglutamine-encoding CAG repeat region (Figure 3B). The shift in reading frame produces a stop codon at nt 435–437, in the middle of the *runt* domain.

The proband in family R (CCD-R) is the only affected member of a family with two siblings. Sequencing of genomic DNA demonstrated heterozygosity for a 10 bp deletion at the end of exon 2, causing a stop codon upstream of the 3′ end of the *runt* domain (Figure 3C).

Family B (CCD-B) is comprised of 27 members with 16 affected individuals, of which 6 were available for genetic analysis. All affected members showed a band of slower mobility in addition to the wild-type band (Figure 3A). One unaffected spouse of an affected member was heterozygous for the wild-type band and a smaller band. Their affected son inherited the larger mutant band from the mother and the smaller band from the father (Figure 3A). The larger band in all affected individuals was due to an in-frame duplication within the polyalanine stretch, leading to a total of 27 alanine residues instead of 17 residues in the wild-type sequence (Figure 3D). The shorter band in the unaffected individual and his affected son was due to an in-frame deletion within the alanine coding region, leading to a total of 11 alanine residues instead of 17. When 160 alleles from unrelated individuals without CCD were amplified and sequenced, 7 alleles were found to code for 11 alanine residues in this region. Therefore, we conclude that the allele with 11 alanines represents a less common, but normal, variant of *CBFA1*.

The affected child in family J (CCD-J) was found to be heterozygous for a G-to-A transition in exon 5 of *CBFA1*. This nucleotide change converts a TGG codon to a TGA (stop) codon and creates a new MboI restriction site (Figure 2D). To confirm its presence in the mutant allele, a 307 bp genomic DNA fragment from this region was amplified using primers I4-F1 and I5-R1 and digested with MboI. As predicted from the sequence, the restriction enzyme cut about half of the amplified DNA from the affected individual into fragments of 82 and 225 bp, whereas amplified DNA from the unaffected parents was not cleaved (Figure 3A).

Discussion

CCD Is Caused by Loss-of-Function Mutations Involving Transcription Factor CBFA1

We identified deletions, insertions, and a missense mutation involving the *CBFA1* gene in patients with CCD. The data demonstrate that *CBFA1* mutations segregate with the CCD phenotype and that heterozygous loss of function is sufficient to produce the characteristic clinical findings. Moreover, the data suggest that CBFA1 is essential for normal skeletal development.

CBFA1 belongs to a family of transcription factors, CBFα proteins, that share a common DNA binding region, the *runt* domain. This domain has high homology with Drosophila *runt* (Kania et al., 1990), a pair-rule gene essential for formation of the segmented body pattern (Nüsslein-Volhard and Wieschaus, 1980). The *runt* domain of CBFα proteins allows dimerization with CBFβ, a ubiquitously expressed nuclear factor that itself does not bind DNA but increases affinity for CBFα binding sites (Ogawa et al., 1993a). Other members of the CBFA family include CBFA2 (AML1) and CBFA3 (AML2) and their mouse homologs PEBP2αA and PEPB1αB. The CBFα/PEBPα/AML factors have been implicated in myeloid cell-specific gene expression (Liu et al., 1993; Ogawa et al., 1993b; Bae et al., 1994; Okuda et al., 1996; Wang et al., 1996). In contrast, CBFA1 appears to be an early marker for the osteoblastic lineage (Ducy et al., 1997).

With the exception of the in-frame expansion of the polyalanine stretch in family B, all the mutations we describe should lead to partial or complete loss of CBFA1 protein domains. Affected individuals in pedigrees O, H, and M are heterozygous for a complete loss of CBFA1 protein. In family G, the insertion of 16 nt within the polyglutamine domain causes a stop codon in the middle of the *runt* domain. In family R, deletion of 10 nt within the *runt* domain causes a stop codon immediately downstream of the deletion. Thus, the protein products of the mutant alleles in CCD-G and CCD-R lack part of the region for DNA binding and dimerization with CBFβ. The mutant proteins would also lack the transactivation domain downstream of the *runt* domain (Bae et al., 1994). The patient in pedigree J has a missense mutation in this C-terminal region. Although the *runt* domain is not affected in this patient, we suggest that the missing 223 C-terminal amino acid residues of the protein result in loss of function.

Affected Individuals in Family B Have an Unusual Phenotype Associated with an Unusual Mutation

Affected individuals in family B have an uncommon phenotype, with minor craniofacial features of CCD but associated with brachydactyly of hands and feet (Figure 4). This may reflect a partial loss of function of the mutant *CBFA1* allele, combined with gain of an abnormal function. The mutation in this family is reminiscent of the expansion of the polyalanine stretch in HOXD13 in human synpolydactyly (Muragaki et al., 1996). It is possible that imperfect triplet repeats cause misalignment of elements during replication followed by mismatch repair that in turn leads to a duplication, as observed in *HOXD13* in synpolydactyly, or a deletion, as observed in *Hoxa13* in hypodactyly (Mortlock et al., 1996). A similar mechanism is likely the basis for the mutation in patient CCD-G.

Loss of CBFA1 Function Affects both Membranous and Endochondral Bone Formation

During embryogenesis, bones develop either by direct formation from osteoblastic progenitor cells or within a temporary framework of hyaline cartilage (for review, see Erlebacher et al., 1995). The direct formation of bone from osteoblastic progenitors produces the flat bones of the skull and part of the clavicle and mandible; the same process occurs in areas of appositional growth of long bones through differentiation of periosteal stem cells into osteoblasts. Endochondral bone formation involves the proliferation and differentiation of chondrocytes and their replacement by osteocytes. The defective membranous bone formation in CCD is consistent

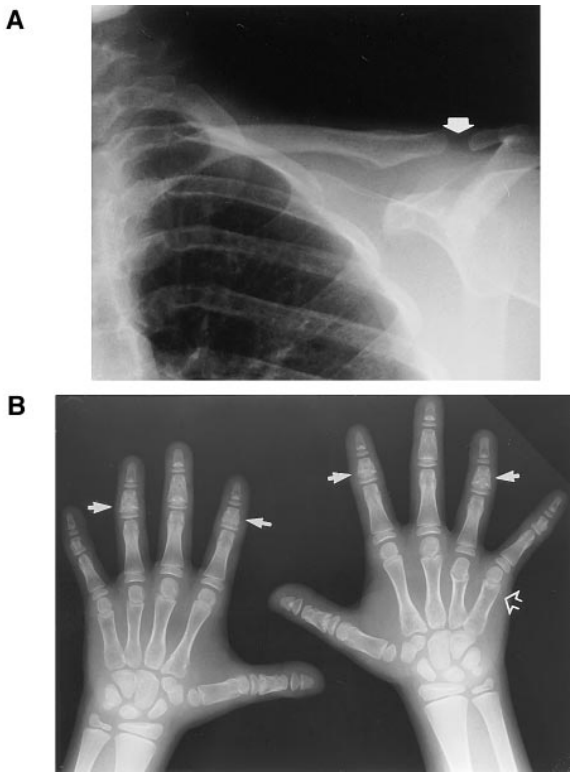

Figure 4. Radiographs of Clavicle and Hands of Affected Individuals in Family CCD-B

(A) Left shoulder region with distal gap in clavicle (arrow).

(B) Affected child with prominent brachydactyly: distal phalanges are hypoplastic and middle phalanges have cone-shaped epiphyses (arrows). Metacarpals exhibit pseudoepiphyses and shortening of metacarpals IV and V (open arrow).

with a key role for CBFA1 in osteoblast differentiation. Stunted growth and metaphyseal changes seen in patients with CCD also suggest, however, that CBFA1 is important for endochondral bone formation.

Recent studies suggest that differentiation of chondrocytes to hypertrophy is regulated by signals between the periosteum and the chondrocytes (Vortkamp et al., 1996). We speculate that CBFA1 is directly or indirectly involved in this signaling process. During the establishment of the ossification centers of long-bone anlagen, periosteal cells differentiate into osteoblasts, and a bone collar is formed around the cartilage. At the same time, chondrocytes differentiate into hypertrophic cells. We suggest that the action of CBFA1 in the perichondrium is necessary for differentiation of chondrocytes to hypertrophy in the underlying cartilage, both at the time of establishment of ossification centers as well as during longitudinal growth, when chondrocytes differentiate to hypertrophy in the growth plates.

In the clavicle, the two mechanisms of bone formation are combined to form the clavicular anlagen (Huang et al., submitted). It is possible that the unique combination of endochondral and intramembranous bone formation as observed in the clavicles renders these bones especially prone to defects in the *CBFA1* gene. The expression of CBFA1 in mesenchymal progenitor cells (Ducy et al., 1997) makes it likely that CBFA1 is not only involved in osteoblastic and chondrocytic differentiation but also in early patterning. This would explain structural defects seen in the Ccd mouse, such as absent deltoid tuberosity and hypoplastic scapulae (Sillence et al., 1987).

Analogies between murine and human skeletal dysplasias have been described (see Mundlos and Olsen, 1997a, 1997b). However, in few instances were the similarities as striking as they are in the *Cbfa1* knockout mouse, the Ccd mouse, and human CCD. The similarities extend beyond the major anomalies, such as hypoplastic clavicles and open fontanelles, to more subtle findings, such as Wormian bones, bell-shaped thorax, hypoplastic scapulae, and dysplastic pubic bones. Supernumerary teeth do not occur in Ccd mice. This can be explained by the fact that mice have only one set of teeth; furthermore, primary teeth are not affected in humans. Phenotypic similarities are accompanied by similar mutational mechanisms. The radiation-induced murine mutant Ccd is deleted around the *Cbfa1* locus (Otto et al., 1997). The localization and extent of the missing segment is comparable to the deletions described for CCD patients (Figure 2). In both mice and men (family O, patients H and M), the *TCTE1* gene is intact, and the deletion extends proximally to include *CBFA1*.

Why mutations in *CBFA1* should cause supernumerary teeth is not obvious. CBFA1 could be involved at several steps during tooth development. The intriguing loss of control of tooth number in CCD clearly deserves further study.

Experimental Procedures

Patients

Members of CCD families were evaluated for the typical signs of CCD. At the time of evaluation, a blood sample was obtained for genetic analysis. All studies were carried out with informed consent of the participating families.

Haplotype Analysis

Polymorphic markers localized to the CCD region (Figure 2A) were amplified by PCR with DNA from members of CCD families. Haplotypes were constructed manually, assuming a minimum number of recombinations in each family. The order of the markers was based on both mapping data for the YAC contig and recombination events observed in the families.

Physical Mapping of the CCD Region

A YAC contig using the CEPH Mega-YAC library was generated to cover the region of interest between the recombinant markers D6S438 and D6S282. YAC clones were identified based on their STS content or by fingerprinting data as determined at the Whitehead Institute, MIT, or CEPH. Individual clones were obtained from CEPH or Research Genetics (Alabama). The presence of known STSs within the CCD locus was tested by PCR amplification or Southern blot analysis. Positive YACs were tested by FISH for chimerism. A total of 20 YACs were tested; 14 were nonchimeric and used to construct the contig.

To determine the sizes and restriction maps of YAC clones, we performed pulsed-field gel electrophoresis in 1% Seakem agarose (FMC) in 0.5× TBE using the CHEF DRII Mapper (Bio–Rad). Agarose plugs of yeast cells were prepared as described by Birren and Lai (1993). Gels were blotted onto Amersham NT^+ Nylon membranes by alkaline blotting, UV cross-linked, and baked for 2 hr at 80°C.

A PAC contig covering the *CBFA1* gene was generated by screening an arrayed human PAC library (Lehrach et al., 1990; Ioannou et al., 1994) with an 800 bp HindIII–EcoRI fragment of the murine *Cbfa1* cDNA corresponding to exons 4–7, as well as with a PCR product corresponding to the *runt* domain that was amplified from murine cDNA using primers AML3F1 and AML3R3 (see below).

Genomic Structure and Sequence of *CBFA1*

The cDNA sequence of *CBFA1* was determined by a combination of nested RT–PCR with lymphoblast RNA and genomic sequencing of PAC clones. For analysis of lymphoblast RNA, PCR primers were designed to amplify the 1.4 kb cDNA in 2 overlapping fragments, from the start of the *runt* domain in exon 1 to the stop codon in exon 7. The primers for the first/second round PCR were AML3F1/AML3F2 and CBFA-7/CBFA-6, respectively. In the second round, the 5′ or 3′ primer was replaced by AML3F5 or AML3R4, respectively.

The characterization of the 5′ end of *CBFA1*, as well as all the intron–exon boundaries, were determined by direct sequencing (using an ABI sequencer) of PAC clones with appropiate exon primers. These primers were derived from published sequences, by the sequencing of RT–PCR products, or from conserved segments in the mouse.

The primers used were as follows: for exon 0, AML3F8 (sense) 5′-GAGAATGCTAACTCGCCTCCAG and AML3R8 (antisense) 5′-GAGACCACCCGAGTCAGTGAGTCG; for exon 1, CBFA-8 (antisense) 5′-CATGGTGCGGTTGTCGTGG, CBFA-9 (sense) 5′-CCACG ACAACCGCACCATG, MCBFA-1 (sense) 5′-ATGCGTATTCCTGTAG ATCCG, and MCBFA-3 (sense) 5′-AGCGACGTGAGCCCGGTG; for exon 2, AML3F2 (sense) 5′-CGGAGAGGTACCAGATGGGAC and AML3R1 (antisense) 5′-GTCCCATCTGGTACCTCTCCG; for exon 3, AMLF3F3 (sense) 5′-TCCCCAAGTAGCTACCTATCA and AML3R2 (antisense) 5′-TGATAGGTAGCTACTTGGGGA; for exon 4, AML3F4 (sense) 5′-ACAAATCCTCCCCAAGTAGCT and AML3R3 (antisense) 5′-CTCATACTGGGATGAGGAATG; for exon 5, AML3F5 (sense) 5′-TACCACCCCGCTGTCTTCCAC and AML3R4 (antisense) 5′-GAAAT GCGCCTAGGCACATCG; for exon 6, AML3F7 (sense) 5′-ATGATGA CACTGCCACCTCTG and AML3R7 (antisense) 5′-TGCCTGGCTCTT CTTACTGAG; for exon 7, AML3R5 (antisense) 5′-GGTTGGAGAAGC GGCTCTCAG, CBFA-6 (antisense) 5′-CACTGGGCCACTGCTGAG, and CBFA-7 (antisense) 5′-GATACGTGTGGGATGTGGC.

Deletion Detection

Deletions were detected by testing polymorphic markers D6S459, D6S452, and D6S271 for loss of heterozygosity. The size of the deletions was estimated by FISH. Purified DNAs from YACs were amplified by inter-Alu PCR using primers AGK34 (Baldini et al., 1992), Alu 3′, and Alu 5′ (Tagle and Collins, 1992). The amplified products were labeled by nick translation with either digoxigenin 11-dUTP or biotin 16-dUTP (Knoll and Lichter, 1994). The digoxigenin-labeled probe was detected with 3 μg/ml rhodamine-conjugated digoxigenin antibody (Boehringer Mannheim), and the biotin-labeled probe with 7 μg/ml fluorescein-conjugated avidin (Vector Laboratories). Chromosomes were counterstained with DAPI. Ten or more hybridized metaphases were scored for each YAC hybridization.

Mutation Detection

Mutation detection was performed by fluorescent sequencing of either genomic PCR or RT–PCR products; poly(A)$^+$ RNA for RT–PCR was prepared from lymphoblastoid cell lines. To confirm heterozygous changes, the PCR product was subcloned in pBluescript vectors, and 10 individual clones were sequenced. The following primers were used: for exon 1, MCBFA3 and CBFA8 (see above); for exon 2, I1-F2 (sense) 5′-CAGATGCTTGATTCCTGTCGG and I2-R1 (antisense) 5′-GTGCTGATTTGTATACAGACTAG; for exon 3, I2-F2 (sense) 5′-TCATTGCCTCCTTAGAGATGC and I3-R2 (antisense) 5′-GGACATGAAAGTGACACTAAC; for exon 4, I3-F2 (sense) 5′-AATGC TGGCCACCAGATACCG and I4-R2 (antisense) 5′-AATAAGCCGCTT CACAGCTCC; for exon 5, I4-F1 (sense) 5′-TAAGGCTGCAATGGTTG CTAT and I5-R1 (antisense) 5′-GTCACTGTGAGCATGGATGAG; for exon 6, I5-F1 (sense) 5′-TAGAACATTAGAGCTGGAAGG and I6-R1 (antisense) 5′-CGGACAGTAACAACCAGACAG; for exon 7, CBFA-10 (sense) 5′-GGAAGTTTACGTGGTCAGTG and CBFA-6 (see above). For primers MCBFA3/CBFA-8, 10% DMSO was added to the PCR reaction.

Acknowledgments

Correspondence should be addressed to S. M. (e-mail: mundlos@winni.kinder.klinik.uni-mainz.de). The project was supported by grants from Deutsche Forschungsgemeinschaft (S. M. and F. O.), NIH grants AR 36819 and AR 35820 (B. R. O.), NIH grant HD 18658 (J. H. M. K.), Beth Israel Pathology Foundation, Inc. (J. H. M. K.), MRC Canada (W. G. C.), The Samuel Lunenfeld Foundation (W. G. C.), and by Organogenesis, Inc. (B. R. O.). We thank Y. Ito for the kind gift of murine *Cbfa1* cDNA, Dr. V. Tiziani for help in collecting some of the human samples, and L. White, I. Quack, K. Geiger, and M. Follo for technical assistance. We thank Drs. R. S. Ramesar, P. H. Beighton, G. Karsenty, and M. Warman for sharing unpublished data and helpful discussions. We are grateful to all patients and family members who participated in the study. Y. Pittel provided expert secretarial assistance.

Received February 27, 1997; revised April 21, 1997.

References

Bae, S.C., Ogawa, E., Maruyama, M., Oka, H., Satake, M., Shigesada, K., Jenkins, N.A., Gilbert, D.J., Copeland, N.G., and Ito, Y. (1994). PEBP2 alpha B/mouse AML1 consists of multiple isoforms that possess differential transactivation potentials. Mol. Cell. Biol. *14*, 3242–3252.

Baldini, A., Ross, M., Nizetic, D., Vatcheva, R., Lindsay, E.A., Lehrach, H., and Siniscalco, M. (1992). Chromosomal assignment of human YAC clones by fluorescence in situ hybridization: use of single-yeast-colony PCR and multiple labeling. Genomics *14*, 181–184.

Birren, B., and Lai, E. (1993). Pulsed Field Gel Electrophoresis. A Practical Guide (New York: Academic Press, Inc.), pp. 49–50.

Ducy, P., Zhang, R., Geoffroy, V., Ridall, A.L., and Karsenty, G. (1997). Osf2/Cbfa1: a transcriptional activator of osteoblast differentiation. Cell, this issue.

Erlebacher, A., Filvaroff, E.H., Gitelman, S.E., and Derynck, R. (1995). Toward a molecular understanding of skeletal development. Cell *80*, 371–378.

Ioannou, P.A., Amamiya, C.T., Garnes, J., Kroisel, P.M., Shizuya, H., Chen, C., Batzer, M.A., and de Jong, P.J. (1994). A new bacteriophage P1-derived vector for the propagation of large human DNA fragments. Nature Genet. *6*, 84–89.

Jones, K.L. (1997). Smith's Recognizable Patterns of Human Malformation, 5th Ed. (Philadelphia: W.B. Saunders Company).

Kania, M.A., Bonner, A.S., Duffy, J.B., and Gergen, J.P. (1990). The Drosophila segmentation gene runt encodes a novel nuclear regulatory protein that is also expressed in the developing nervous system. Genes Dev. *4*, 1701–1713.

Knoll, J.H.M., and Lichter, P. (1994). In situ hybridization to metaphase chromosomes and interphase nuclei. In Current Protocols in Human Genetics, N.C. Dracopoli, J.L. Haines, B.R. Korf, D.T. Moir, C.C. Morton, C.E. Seidman, J.G. Seidman, and D.R. Smith, eds. (New York: Green-Wiley), Unit 4.3.

Kwiatkowski, T.J., Jr., Beaudet, A.L., Trask, B.J., and Zoghbi, H.Y. (1991). Linkage mapping and fluorescence in situ hybridization of TCTE1 on human chromosome 6p: analysis of dinucleotide polymorphisms on native gels. Genomics *10*, 921–926.

Ledley, F.D., Lumetta, M.R., Zoghbi, H.Y., VanTuinen, P., Ledbetter, S.A., and Ledbetter, D.H. (1988). Mapping of human methylmalonyl CoA mutase (MUT) locus on chromosome 6. Am. J. Hum. Genet. *42*, 839–846.

Lehrach, H., Drmanac, R., Hoheisel, J., Larin, Z., Lennon, G., Monaco, A.P., Nizetic, D., Zehelner, G., and Poustka, A. (1990). Hybridization fingerprinting in genome mapping and sequencing. In Genetic and Physical Mapping, K.E. Davies and S.M. Tilghman, eds. (Cold

Spring Harbor, New York: Cold Spring Harbor Laboratory Press), pp. 39–81.

Levanon, D., Negreanu, V., Bernstein, Y., Bar-Am, I., Avivi, L., and Groner, Y. (1994). AML1, AML2, and AML3, the human members of the runt domain gene-family: cDNA structure, expression, and chromosomal localization. Genomics *23*, 425–432.

Liu, P., Tarle, S.A., Hajra, A., Claxton, D.F., Marlton, P., Freedman, M., Siciliano, M.J., and Collins, F.S. (1993). Fusion between transcription factor CBF beta/PEBP2 beta and a myosin heavy chain in acute myeloid leukemia. Science *261*, 1041–1044.

Merriman, H.L., von Wijnen, A.J., Hiebert, S., Bidwell, J.P., Fey, E., Lian, J., Stein, J., and Stein, G.S. (1995). The tissue-specific nuclear matrix protein, NMP-2, is a member of the AML/CBF/PEBP2/Runt domain transcription factor family: interactions with the osteocalcin gene promoter. Biochemistry *34*, 13125–13132.

Miyoshi, H., Ohira, M., Shimizu, K., Mitani, K., Hirai, H., Imai, T., Yokoyama, K., Soeda, E., and Ohki, M. (1995). Alternative splicing and genomic structure of the AML1 gene involved in acute myeloid leukemia. Nucleic Acids Res. *23*, 2762–2769.

Mortlock, D.P., Post, L.C., and Innis, J.W. (1996). The molecular basis of hypodactyly (Hd): a deletion in Hoxa13 leads to arrest of digital arch formation. Nature Genet. *13*, 284–289.

Mundlos, S., Mulliken, J.B., Abramson, D.L., Warman, M.L., Knoll, J.H., and Olsen, B.R. (1995). Genetic mapping of cleidocranial dysplasia and evidence of a microdeletion in one family. Hum. Mol. Genet. *4*, 71–75.

Mundlos, S., and Olsen, B.R. (1997a). Heritable diseases of the skeleton. Part I: molecular insights into skeletal development-transcription factors and signaling pathways. FASEB J. *11*, 125–132.

Mundlos, S., and Olsen, B.R. (1997b). Heritable diseases of the skeleton. Part II: molecular insights into skeletal development-matrix components and their homeostasis. FASEB J., *11*, 227–233.

Muragaki, Y., Mundlos, S., Upton, J., and Olsen, B.R. (1996). Altered growth and branching patterns in synpolydactyly caused by mutations in HOXD13. Science *272*, 548–551.

Nienhaus, H., Mau, U., Zang, K.D., and Henn, W. (1993). Pericentric inversion of chromosome 6 in a patient with cleidocranial dysplasia. Am. J. Med. Genet. *46*, 630–631.

Nüsslein-Volhard, C., and Wieschaus, E. (1980). Mutations affecting segment number and polarity in Drosophila. Nature *287*, 795–801.

Ogawa, E., Inuzuka, M., Maruyama, M., Satake, M., Naito-Fujimoto, M., Ito, Y., and Shigesada, K. (1993a). Molecular cloning and characterization of PEBP2 beta, the heterodimeric partner of a novel Drosophila runt-related DNA binding protein PEBP2 alpha. Virology *194*, 314–331.

Ogawa, E., Maruyama, M., Kagoshima, H., Inuzuka, M., Lu, J., Satake, M., Shigesada, K., and Ito, Y. (1993b). PEBP2/PEA2 represents a family of transcription factors homologous to the products of the Drosophila runt gene and the human AML1 gene. Proc. Natl. Acad. Sci. USA *90*, 6859–6863.

Okuda, T., van Deursen, J., Hiebert, S.W., Grosveld, G., and Downing, J.R. (1996). AML1, the target of multiple chromosomal translocations in human leukemia, is essential for normal fetal liver hematopoiesis. Cell *84*, 321–330.

Otto, F., Thormell, A.P., Crompton, T., Denzel, A., Gilmour, K.C., Rosewell, I.R., Stamp, G.W.H., Beddington, R.S.P., Mundlos, S., Olsen, B.R., Selby, P.B., and Owen, M.J. (1997). *Cbfa1*, a candidate gene for the Cleidocranial Dysplasia syndrome, is essential for osteoblast formation and bone development. Cell, this issue.

Selby, P.B., and Selby, P.R. (1978). Gamma-ray-induced dominant mutations that cause skeletal abnormalities in mice. II. Description of proved mutations. Mut. Res. *51*, 199–236.

Sillence, D.O., Ritchie, H.E., and Selby, P.B. (1987). Animal model: skeletal anomalies in mice with cleidocranial dysplasia. Am. J. Med. Genet. *27*, 75–85.

Tagle, D.A., and Collins, F.S. (1992). An optimized Alu-PCR primer pair for human-specific amplification of YACs and somatic cell hybrids. Hum. Mol. Genet. *1*, 121–122.

Vortkamp, A., Lee, K., Lanske, B., Segre, G.V., Kronenberg, H.M., and Tabin, C.J. (1996). Regulation of rate of cartilage differentiation by Indian hedgehog and PTH-related protein. Science *273*, 613–622.

Wang, Q., Stacy, T., Binder, M., Marin-Padilla, M., Sharpe, A.H., and Speck, N.A. (1996). Disruption of the Cbfa2 gene causes necrosis and hemorrhaging in the central nervous system and blocks definitive hematopoiesis. Proc. Natl. Acad. Sci. USA *93*, 3444–3449.

GenBank Accession Number

The GenBank accession numbers for the CBFA1 sequences reported here are: AF001443, AF001444, AF001445, AF001446, AF001447, AF001448, AF001449, and AF001450.